

Supporting Information

From Langmuir Blodgett to Grafted Films

M. Gabaji ^a, J. Médard ^b, A. Hemmerle ^c, J. Pinson ^{b,*}, J. P. Michel ^{a,*}

^a Université Paris-Saclay, CNRS, Institut Galien Paris Sud, 92296, Châtenay-Malabry, France.

^b Université de Paris, ITODYS, CNRS, UMR 7086, 15 rue J-A de Baïf, F-75013 Paris, France

^c Synchrotron SOLEIL, L'Orme des Merisiers, Saint Aubin, BP48, Gif-sur-Yvette CEDEX, France.

*Corresponding author: jean.pinson@univ-paris-diderot.fr or jeanphilippe.michel@universite-paris-saclay.fr

10 pages, 13 figures, 2 tables.

Image of the modified Langmuir trough

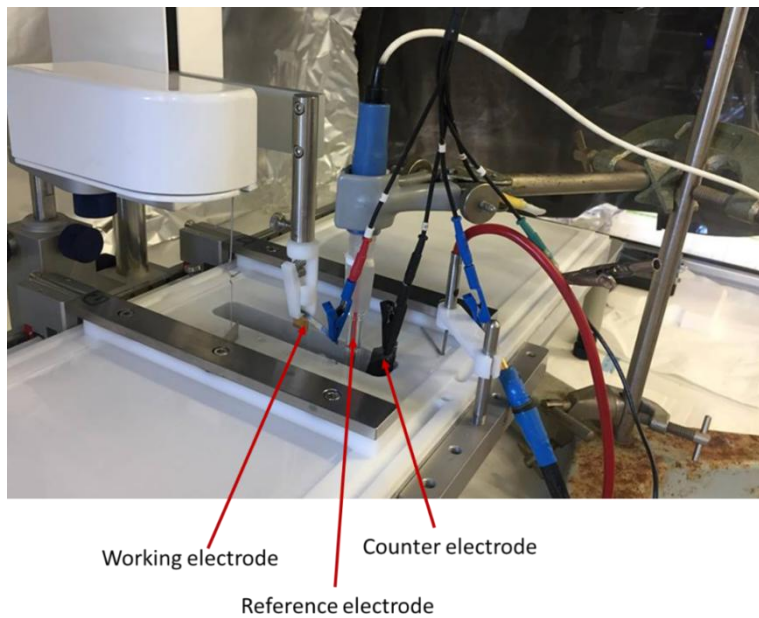


Fig. SI-1: image of the modified Langmuir trough for LB-eG process.

Electrografting of ODA on gold

Electrochemical oxidation of ODA on gold.

We have measured a voltammogram of ODA in different solvents. In ACN (Fig. SI-2) the adsorption of ODA blocks the electrode and reduces the background current.

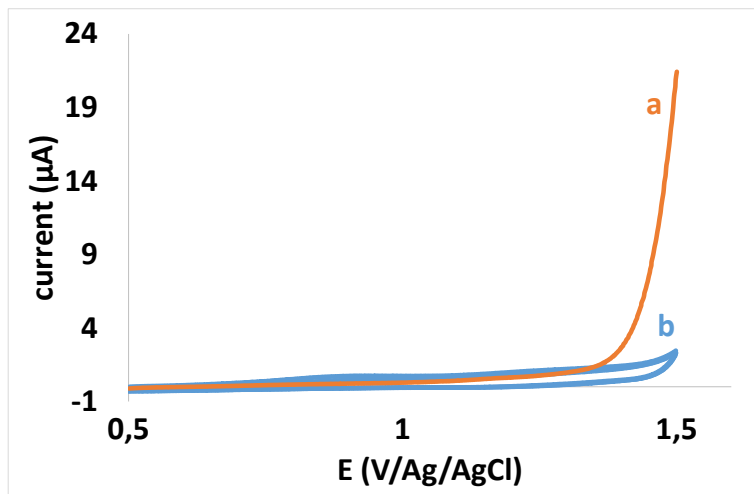


Fig. SI-2: Cyclic voltammogram on an Au electrode a) in $\text{ACN} + 0.1 \text{ M } \text{NBu}_4\text{BF}_4$ and b) after addition of a nominal concentration $c = 1 \text{ mM}$ of ODA, scan rate $v = 0.1 \text{ Vs}^{-1}$.

ODA is more soluble in DMF; in DMF + 0.1M NBu₄BF₄, the oxidation peak of Au is observed at Ep = 1.0 V/(Ag/AgCl); and the oxidation wave of ODA is observed as a broad peak at Ep (ODA) = 1.36 V/SCE, the same potential as butylamine (Fig. SI-3).

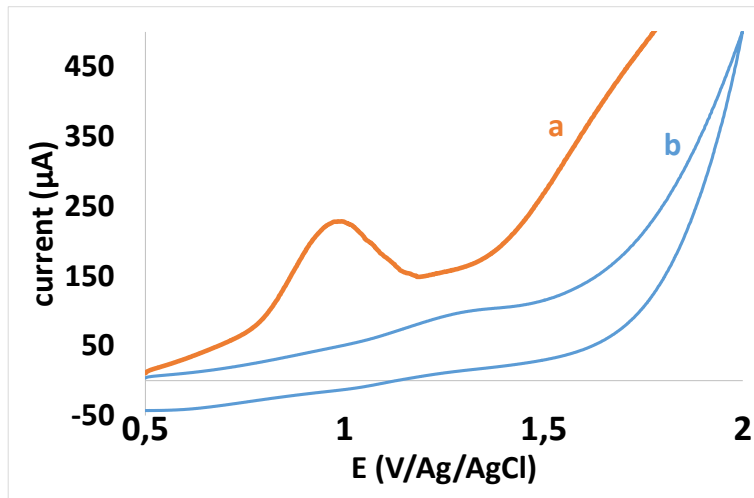


Fig. SI-3: Cyclic voltammogram on an Au electrode a) in DMF + 0.1 M NBu₄BF₄ and b) after addition of ODA (c = 1 mM). Scan rate v = 0.1 Vs⁻¹.

We also recorded the background in the same pH 9 solution used for the formation of the Langmuir film. The onset of the background is about + 0.8 V/SCE (Fig. SI-4).

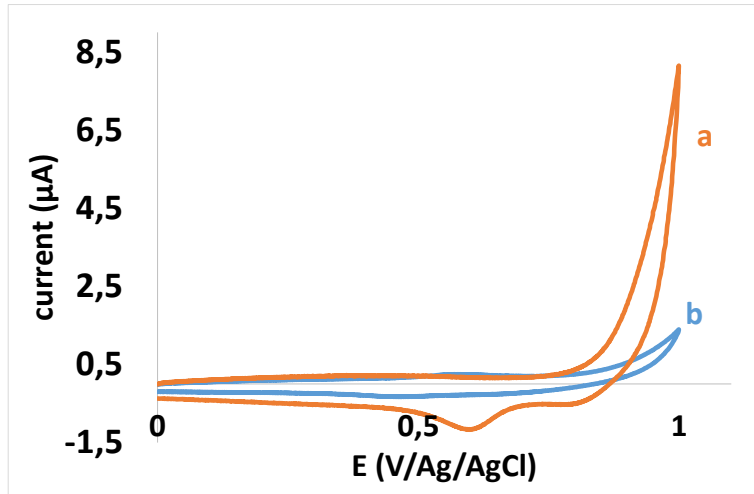


Fig. SI-4: Cyclic voltammogram on an Au electrode a) in a pH 9 solution and b) after addition of ODA (c = 1 mM). Scan rate v = 0.1 Vs⁻¹.

Water contact angle on Au-ODA_{LB-G}.

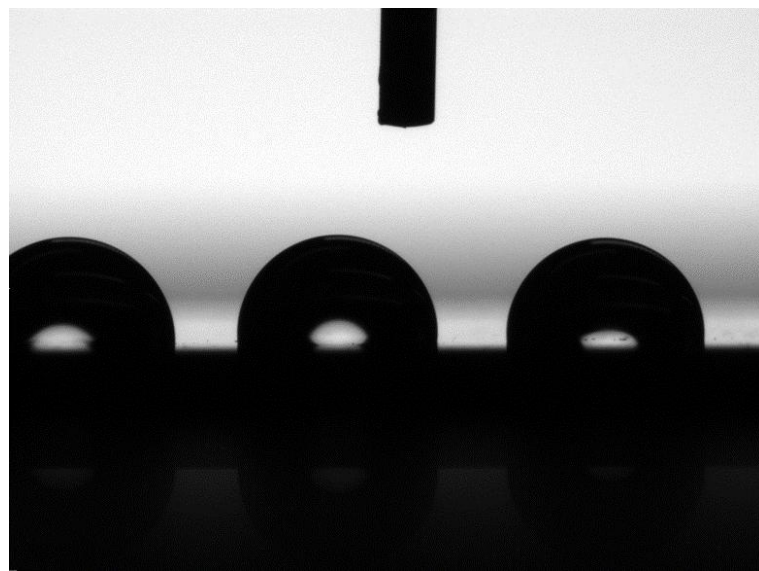


Fig. SI-5: The water contact angle of $Au\text{-ODA}_{LB\text{-G}}$.

The water contact angle of $Au\text{-ODA}_{LB\text{-G}}$ is $101.3^\circ \pm 0.5^\circ$.

Infrared Spectrum of $Au\text{-ODA}_{LB}$.

The stability of $Au\text{-ODA}_{LB}$ film was tested by ultrasonication for 3 min. As shown by the IR spectra in Fig. SI-6, the ODA_{LB} film is mainly desorbed under such conditions. The monolayer dewetting was also confirmed by AFM (data not shown).

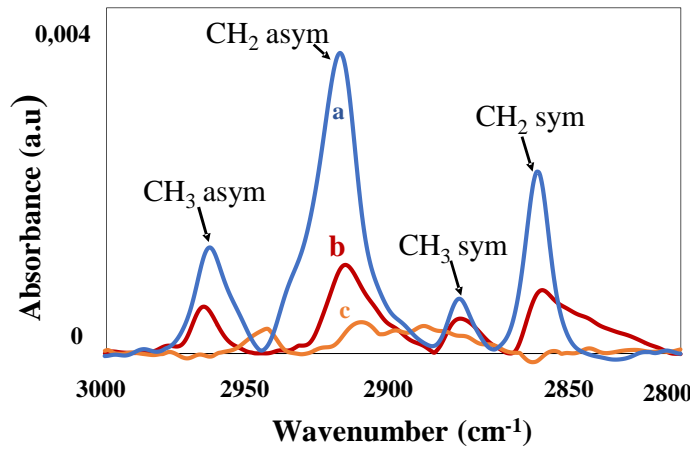
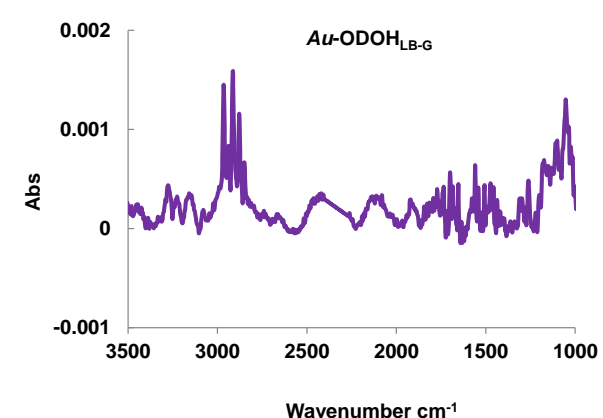
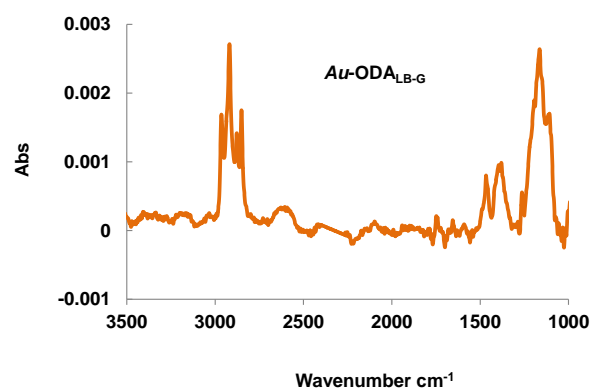
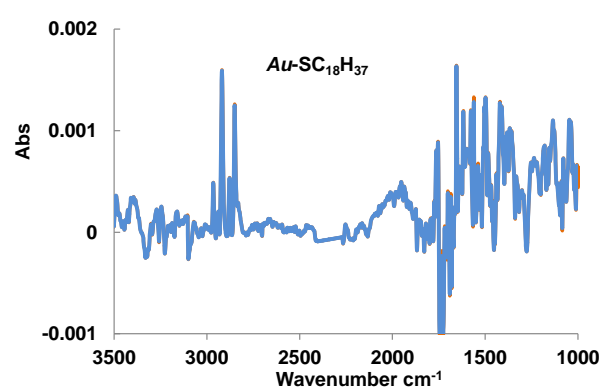
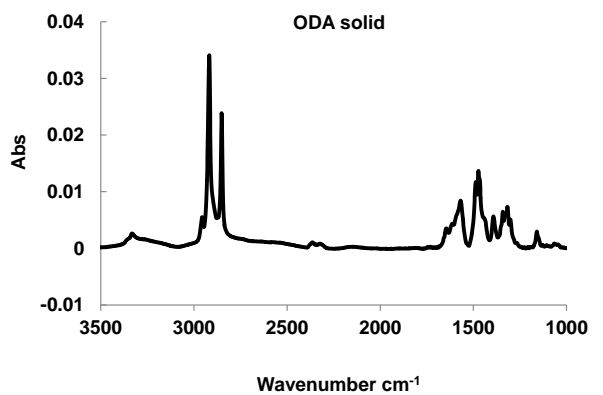


Fig. SI-6: IRRAS spectra of a) $Au\text{-SC}_{18}\text{H}_{37}$, b) $Au\text{-ODA}_{LB}$, c) $Au\text{-ODA}_{LB}$ after ultrasonication.

Infrared Spectra



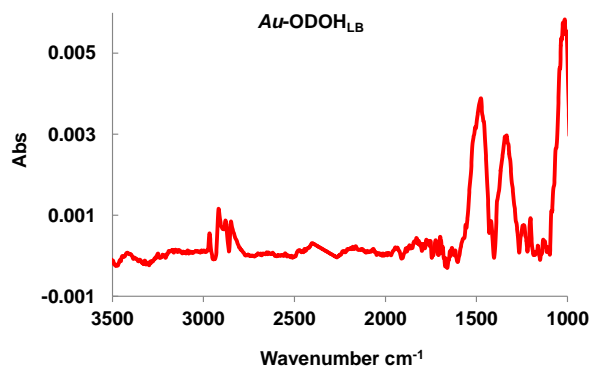


Figure SI-7: Infrared spectra of ODA solid, $Au-SC_{18}H_{37}$, $Au-ODA_{LB-G}$, $Au-ODOH_{LB-G}$ and ODA_{LB} .

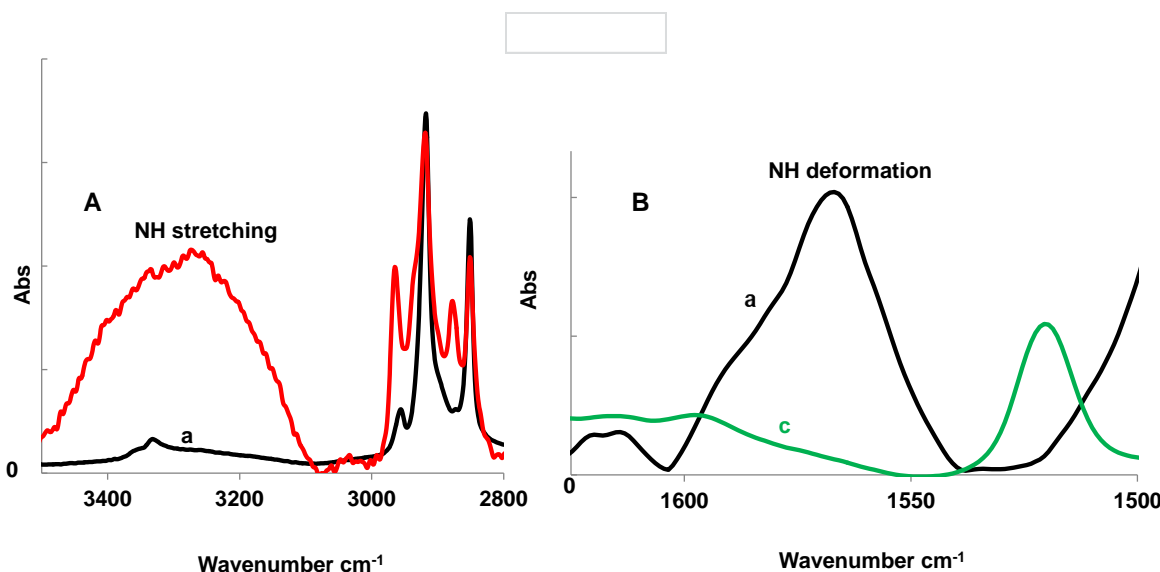


Figure SI-8: A) NH stretching and B) deformations vibrations of a) solid ODA, b) $Au-ODA_{LB-G}$, c) $Au-ODA_{LB}$. Normalized spectra, arbitrary absorbance units.

XPS of $Au-ODA_{LB-G}$.

Table SI-1 and the spectra (Fig. SI-8) indicate the presence of Au4f in agreement with a thin film, of the nitrogen of ODA with C1s/N1s ~18 as expected from the chemical formula and of a contamination by O1s.

Table SI-1. XPS of $Au-ODA_{LB-G}$.

| Atom | Binding Energy (eV) | Atomic proportions % |
|------|---------------------|----------------------|
| Au4f | 83.9 | 9.5 |
| C1s | 285.2 | 70.8 |
| N1s | 400.4 | 4.0 |

| | | |
|-----|-------|------|
| O1s | 532.6 | 15.7 |
|-----|-------|------|

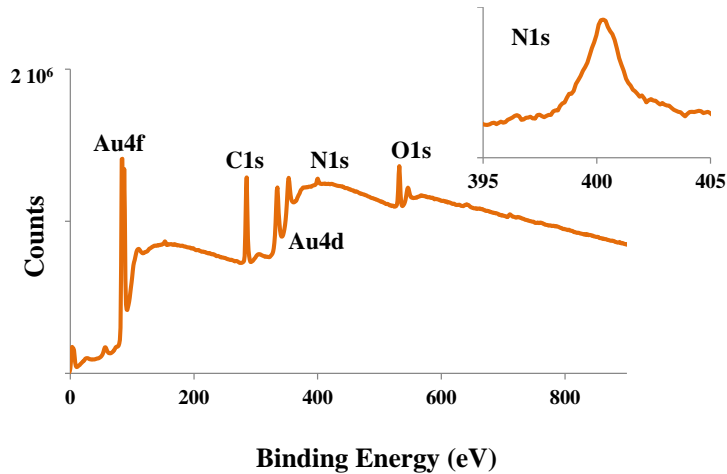


Fig. SI-9: XPS spectrum of $Au\text{-}ODA_{LB\text{-}G}$.

Electrografting of ODOH on gold

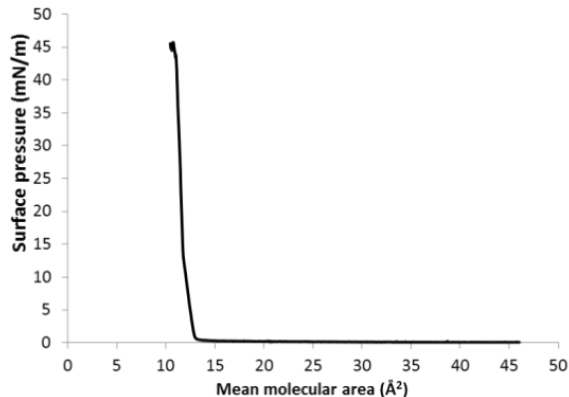


Fig. SI-10: (a) Compression isotherm of ODOH on pH 2 on aqueous solution at 21°C prior to grafting on Au.

Water Contact Angle and thickness of $Au\text{-}ODOH_G$.

The water contact angle $95.7^\circ \pm 1.4^\circ$ and the thickness of the film $1.51\text{ nm} \pm 0.4\text{ nm}$ are similar to that obtained with ODA.

XPS of $Au\text{-}ODOH_{LB\text{-}G}$.

Table SI-2 and the spectrum (Fig. SI-10) indicate the presence of Au4f in agreement with a thin film. Presence of the oxygen of ODOH_G was detected on the surface but also some oxygen and nitrogen contaminations.

Table SI-2. XPS of Au-ODOH_{LB-G}.

| Atom | Binding Energy (eV) | Atomic proportions % |
|------|---------------------|----------------------|
| Au4f | 83.9 | 33.8 |
| C1s | 285.2 | 51.6 |
| N1s | 400.4 | 1.0 |
| O1s | 532.6 | 13.6 |

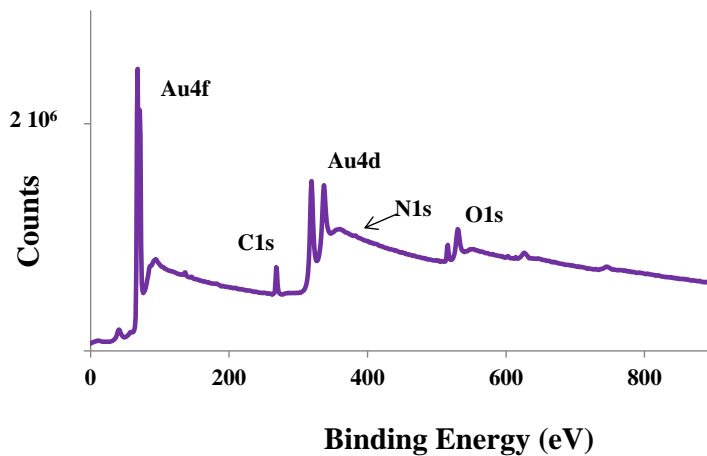


Fig. SI-11: XPS spectrum of Au-ODOH_{LB-G}.

AFM images of Au-ODOH_{LB-G}.

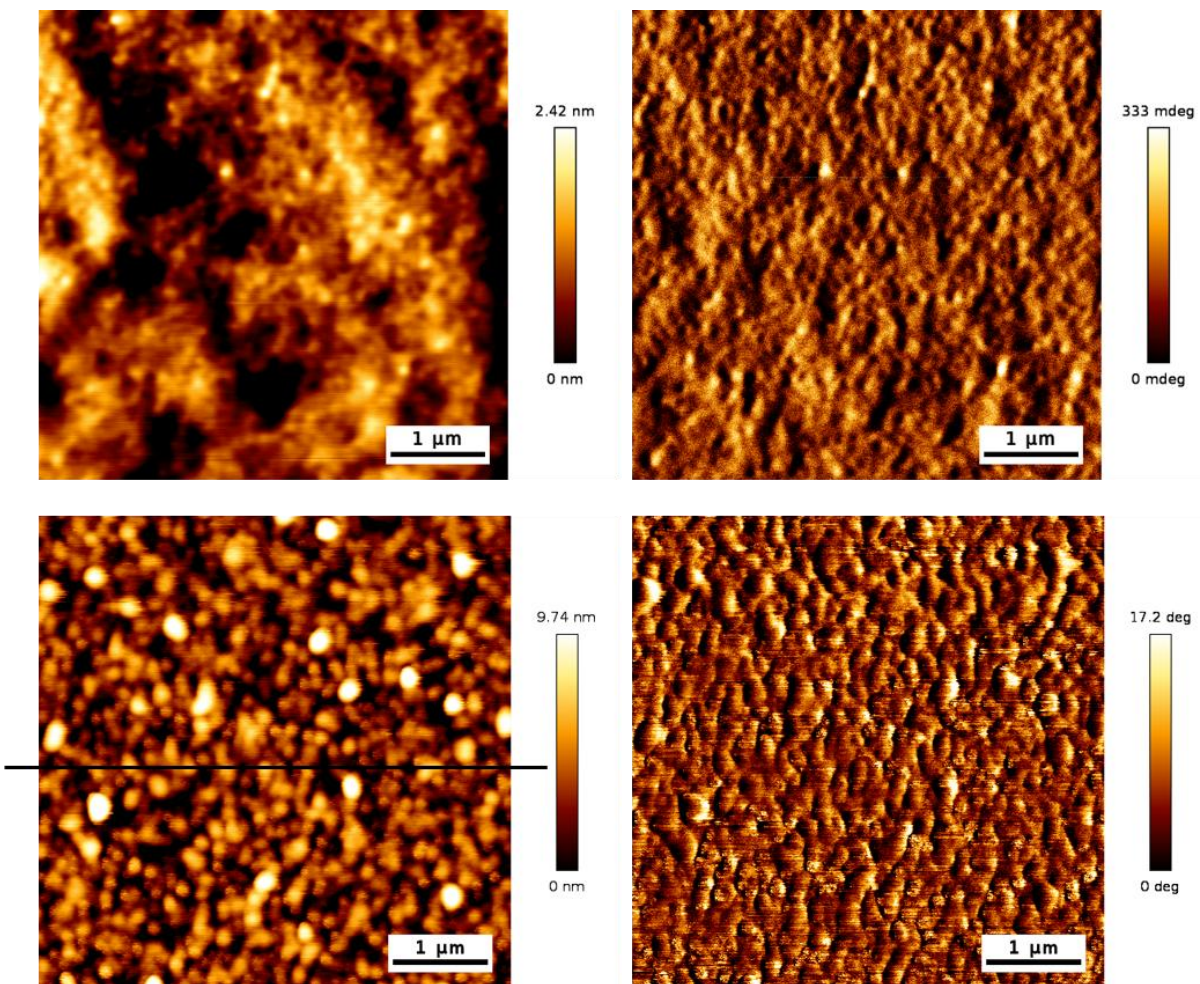


Fig. SI-12: AFM images of Au-ODOH_{LB-G}.

Fig. SI-11 presents AFM height (left) and phase (right) images of (upper images) bare Au surface before LB-eG process of ODOH and of (lower images) Au-ODOH_{LB-G} after ODOH LB-eG process on Au surface. The surface appears very rough after transfer: numerous small round shaped aggregates with 3 to 5 nm heights cover the gold surface. Among them, some are higher, up to 10 nm height.

IRRAS of Au-ODOH_{LB-G}.

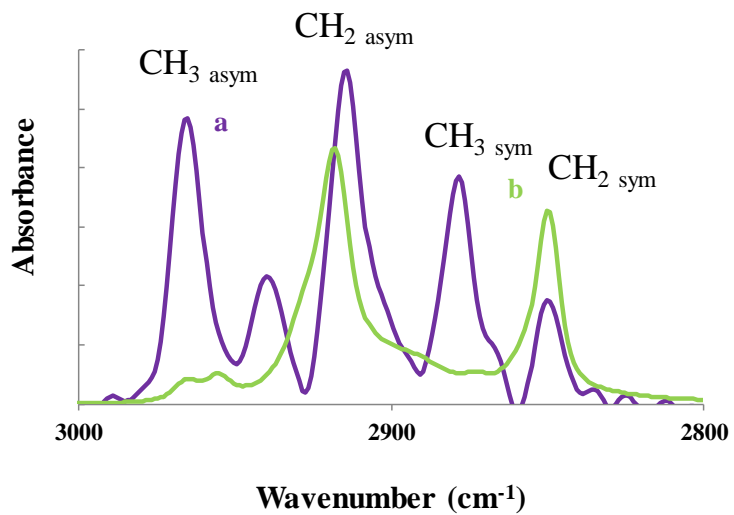


Fig. SI-13: IRRAS spectra of a) Au-ODOH_{LB-G}, b) Au-ODOH solid. Normalized spectra, arbitrary absorbance units.